Research article

Nematicidal activity and action mode of a methyl-accepting chemotaxis protein from *Pseudomonas syringae* against *Caenorhabditis elegans*

Jiaoqing Li [a,1], Haiyan Dai [b,1], Anum Bashir [b,1], Zhiyong Wang [b], Yimin An [c], Xun Yu [b], Liangzheng Xu [a,**], Lin Li [b,*]

[a] Guangdong Provincial Key Laboratory of Conservation and Precision Utilization of Characteristic Agricultural Resources in Mountainous Areas, School of Life Sciences, Jiaying University, Meizhou 514015, China
[b] National Key Laboratory of Agricultural Microbiology, College of Life Science and Technology, Huazhong Agricultural University, Wuhan 430070, China
[c] Pomelo Engineering Technology Center, School of Life Sciences, Jiaying University, Meizhou 514015, China

A B S T R A C T

The conventional phytopathogen *Pseudomonas syringae* reportedly possesses several virulence determinants against *Caenorhabditis elegans*; however, their action mechanisms remain elusive. This study reports the nematicidal activity and action receptor of a methyl-accepting chemotaxis protein (MCP03) of a wild-type *P. syringae* MB03 against *C. elegans*. Purified MCP03 exhibited nematicidal toxicity against *C. elegans* at a half-lethal concentration of 124.4 μg mL^{-1}, alongside detrimental effects on the growth and brood size of *C. elegans*. Additionally, MCP03-treated worms exhibited severe pathological destruction of the intestine and depressed wrinkles of the cuticle. Yeast two-hybrid assays identified a subunit of COP9 signalosome, namely CSN-5, which functioned as an MCP03 action receptor. *In vitro* pull-down verified the binding interaction between MCP03 and CSN-5. RNA interference assays confirmed that MCP03 antagonizes CSN-5, thereby adversely affecting the brood size and cuticle integrity of *C. elegans*. Following MCP03 infection, the expression of genes related to reproduction, growth, and cuticle formation, such as *kgb-1*, *unc-98*, and *col-117*, was considerably downregulated, indicating pathological changes in MCP03-treated nematodes. Therefore, we proposed that MCP03 antagonizes CSN-5, causing lethality as well as detrimental effects on the fertility, growth, and morphogenesis of *C. elegans*, which can provide new insights into the signaling pathways and mechanisms underlying the nematicidal action of MCP03 toward *C. elegans*.

1. Introduction

Plant-parasitic nematodes (PPNs) are a large group of soil-borne roundworms that mainly attack underground plant parts and cause stunted growth, thereby endangering nutrient supply from the soil and causing a first-hand global annual yield loss of >\$157 billion

[1]. Additionally, these nematodes increase the susceptibility of plant roots to other pathogenic fungal and bacterial infections and serve as vectors for certain plant-pathogenic viruses [2]. Although various chemical nematicides and agricultural management have been the typical implements for controlling PPNs for a long time, integrated biological control has become a prioritized approach in combating PPNs owing to its sustainability and eco-friendly nature [3,4].

Various soil-borne bacteria belonging to several genera, such as *Bacillus* [5,6], *Pseudomonas* [7,8], *Pasteuria* [9], and *Burkholderia* [10], reportedly exhibit potent nematicidal activity. These bacteria have developed various strategies, including the production of external toxins, invasive enzymes, or other active substances, to trap and kill nematodes and act as external parasites by utilizing

Table 1
Bacterial, yeast and nematode strains, plasmids and oligonucleotide primers used in this study.

Strains/plasmids/primers	Phenotypes/sequences [a]	Sources
Bacterial strains		
P. syringae		
MB03	A wild-type strain with high ice-nucleating activity	Li et al.[23]
E. coli		
DH5α	*supE44ΔlacU169(Φ80 lacZΔM15) hdsR17 recA1endA1 gyrA96 thi-1 relA1*	Laboratory stock
BL21(DE3)	F⁻*ompT hsdS (rB⁻mB⁻)* dcm ⁺ Tetr *galλ(DE3) endA* The [*argU proL* Cam^r] [*argU ileY leuW* Strep/Spe^{cr}]	Invitrogen
OP50	Amp^r, uracil auxotroph, Food source used for *C. elegans*	Laboratory stock
HT115(DE3)	Tet^r, an RNase III-deficient *E. coli* strain	CGC [b]
MB830	*E. coli* BL21(DE3) harboring pGEX-6P-1	This study
MB831	*E. coli* BL21(DE3) harboring pMB831	This study
MB833	*E. coli* BL21(DE3) harboring pMB833	This study
MB834	*E. coli* HT115(DE3) harboring pMB834	This study
Yeasts		
Y2Hgold	*MATa, trp1, leu2, ura3, his3, gal4Δ, gal80Δ*	Clontech
Y187	*MATα, ura3, his3, ade2, trp1, Leu2, gal4Δ, met, gal80Δ*	Clontech
MB832	Y2Hgold harboring pMB832	This study
Nematodes		
N2	A wild-type *C. elegans*	CGC
FT63 (*dlg::gfp*)	A GFP-labeled transgenic *C. elegans* expressed (*dlg::gfp*) in epithelial cell junction	CGC
LG333 (*skn-1b::gfp*)	A GFP-labeled transgenic *C. elegans* expressed (*skn-1b::gfp*)	CGC
Plasmids		
pET-28a	Kan^r, *E. coli* expression vector, 5369 bp	Novagen
pMB831	Kan^r, pET28a derivative harboring *mcp03* gene at *Eco*R I/*Xho* I site, 7138 bp	This study
pGBKT7	Amp^r, pGEX-6P-1 derivative harboring *csn-5* gene at *Eco*R I site, 6000 bp	TaKaRa, Inc.
pMB832	Kan^r, pGBKT7 derivative harboring *mcp03* gene at *Nde* I/*Bam*H I sites, 9100 bp	This study
pGADT7-*csn-5*	Amp^r, Y2H expressing csn-5, 9100 bp	This study
pGBKT7-53	Kan^r, Y2H expression vector, positive control plasmid, 8300 bp	TaKaRa, Inc.
pGBKT7-lam	Kan^r, Y2H expression vector, negative control plasmid, 7900 bp	TaKaRa, Inc.
pGEX-6P-1	Amp^r, *E. coli* expression vector, 4900 bp	Novagen
pMB833	Amp^r, pGEX-6P-1 derivative harboring *csn5* gene at *Eco*R I site, 6000 bp	This study
pL4440	Amp^r, *E. coli* expression vector, 2800 bp	Takara
pMB834	Amp^r, pL4440 derivative harboring *csn-5* gene at *Hin*d III site, 3900 bp	This study
Oligonucleotide primers [c]		
F-pET28a-mcp03	5c–CCG<u>GAATTC</u>ATGCAGACGTTAAAGGC–3′	
R-pET28a-mcp03	5′–CCG<u>CTCGAG</u>TTATTTACCCAACAGCAGC–3′	
F-pGBKT7-mcp03	5′–CGC<u>CATATG</u>ATGCAGACGTTAAAGGCTTTG–3′	
R-pGBKT7-mcp03	5′–CGC<u>GGATCC</u>TTATTTACCCAACAGCAGCGC–3′	
F-pGEX-6P-1-csn5	5′–CCCCTGGGATCCCCGGAAATGGAAGTTGATACGTC–3′	
R-pGEX-6P-1-csn5	5′–CCGCTCGAGTCGACCCGGGTTAAGCATCGGCCATCTC–3′	
F-pL4440-csn5	5′–CAGGAATTCGATATCAAGATGGAAGTTGATAACGTC–3′	
R-pL4440-csn5	5′–TCGACGGTATCGATAAGTTAAGCATCGGCCATCTC–3′	
For qRT-PCR		
F-GAPDH	5′–TAACTTCGGTATCATCGAAGGACTC–3′	
R-GAPDH	5′–GACGGAAACATCTGGTGTAGGGA–3′	
F-csn5	5′–TTCGCTCTTCCAGTTGAGGG–3′	
R-csn5	5′–CGACCTTCCGTATCGCACAT–3′	
F-col-117	5′–GGTGTGCGTCACTCTTCCAA–3′	
R-col-117	5′–ACGGTTTCCAGATGGGATGG–3′	
F-mpk-1	5′–TGGACTGGGTGCAAGTGAAG–3′	
R-mpk-1	5′–GCAACGAGCCATCTGAAACC–3′	
F-kgb-1	5′–GACGATGAGGTAAACGCCCC–3′	
R-kgb-1	5′–GTGAAAATGTCGTGGTCGGC–3′	
F-unc-98	5′–AGCAAGAAGCGAGTCCTACC–3′	
R-unc-98	5′–TGCTTCGGCTCGTATCCTTC–3′	

Note.

  [a] Amp^r, ampicillin resistance, Kan^r, kanamycin resistance, Tet^r, tetracycline resistance..

  [b] CGC, *Caenorhabditis* Genetics Center, College of Biological Sciences, University of Minnesota..

  [c] The underlined sequences indicate the restriction enzyme sites..

extracellular proteases to digest the nematode cuticle [11]. In addition, they can produce nematode-toxic metabolites after entering the nematode body; for instance, the Cry proteins from the nematicidal bacterium *Bacillus thuringiensis* formed lytic pores in the cell membrane of intestinal epithelial cells upon ingestion [12].

Chemotaxis is a conventional bacterial behavior that allows them to sense chemical cues in their surroundings, thereby enabling them to relocate to favorable niches away from toxic substances. Methyl-accepting chemotaxis proteins (MCPs) are a family of chemoreceptors responsible for the chemotactic behaviors of numerous bacteria [13]. Moreover, chemotaxis is involved in the
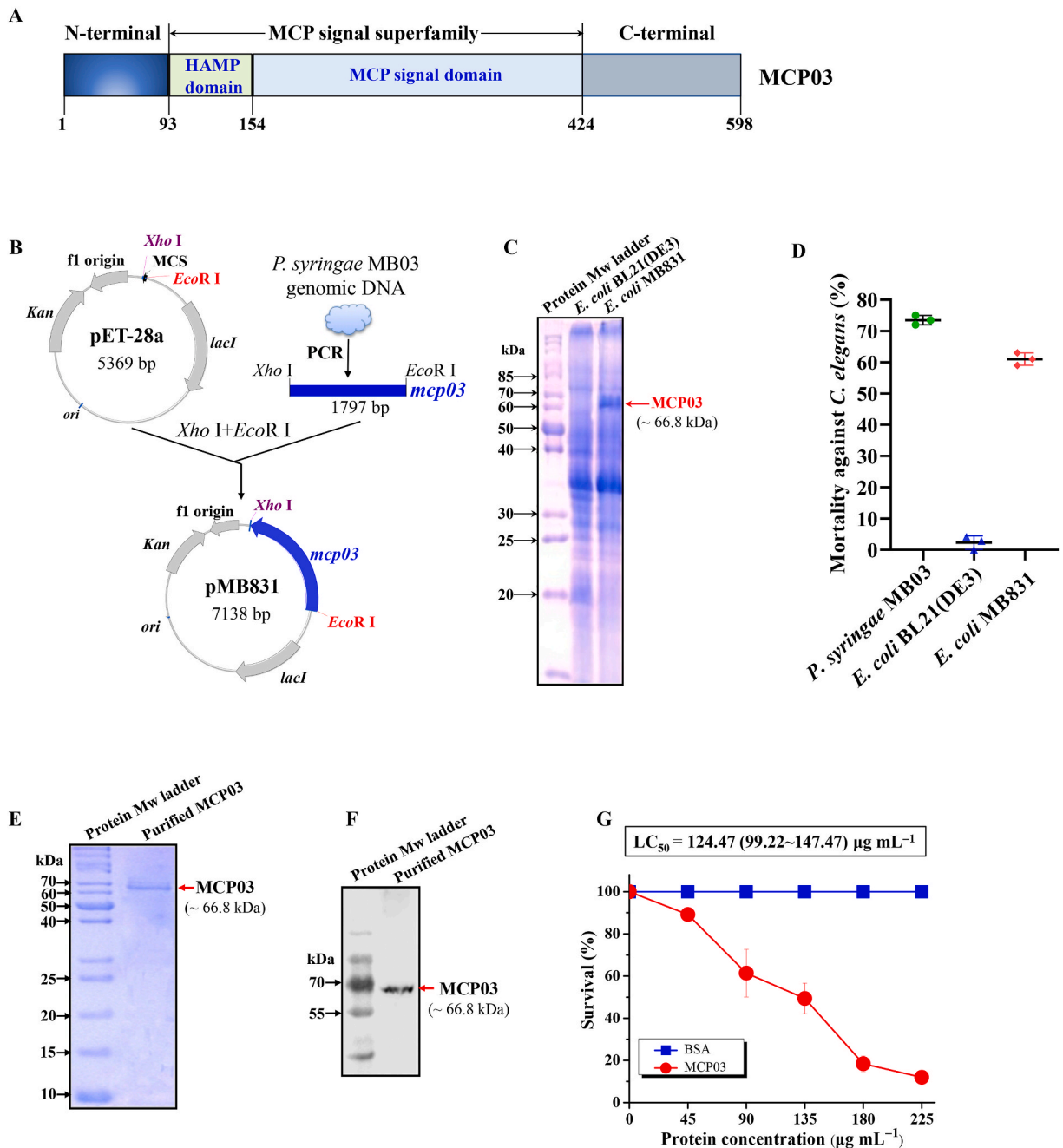

Fig. 1. Expression, structural organization, and nematicidal activity of MCP03. (**A**) Conserved domain analysis of MCP03. (**B**) Schematic representation of the construction of plasmid pMB831 expressing the mcp03 gene. (**C**) SDS–PAGE analysis of whole-cell lysate of recombinant *E. coli* MB831, *E. coli* BL21(DE3) was used as the negative control. (**D**) Whole-cell nematicidal activity of *E. coli* strain MB831 against *C. elegans*. *P. syringae* MB03 and *E. coli* BL21(DE3) were used as the positive and negative control, respectively. (*** indicate $p < 0.001$). (**E**) SDS–PAGE and (**F**) Western blot analysis of purified MCP03 protein. (**G**) Nematicidal activity assay of purified MCP03 protein against *C. elegans*. Error bars represent the standard deviations from the mean of three independent experiments.

pathogenicity of various bacterial pathogens, including *Vibrio cholera* [14], *Coronobacter sakazakii* [15], *Campylobacter jejuni* [16], *Pseudomonas aeruginosa* [16], and *Pseudomonas syringae* [17]. The connection between chemotaxis and pathogenicity relies on the detection of pathogenicity-related signal molecules in the hosts by MCPs, which play a critical role in regulating certain cellular activities, such as biofilm formation, toxin production, exopolysaccharide production, flagellum biosynthesis, cell survival, motility, pathogenicity, and antibiotic resistance [18].

Recently, the conventional phytopathogen *P. syringae* has been reported to exhibit nematicidal activity against the free-living model nematode *Caenorhabditis elegans* [19,20]. In addition, a recent genome-wide prediction analysis also identified several potent nematicidal factors against *C. elegans* in a *P. syringae* wild-type strain MB03, including an MCP (namely MCP03) [21]. The current study aims to elucidate the nematicidal activity and action mechanism of MCP03. Because of the current technical limitations of molecular genetic studies of PPNs, *C. elegans* was employed as a target nematode owing to its well-characterized genetic background [22]. We identified for the first time that a subunit of a COP9 signalosome (CSN) functioned as a receptor protein (namely CSN-5) of MCP03 in *C. elegans*, which may associatively exert destructive effects on the intestinal tract, exhibited lethal and detrimental effects on egg-laying and growth, and surface cuticles by downregulating the expression of genes related to these activities. Therefore, a putative outline mechanism underlying the nematicidal action of MCP03 following its binding with CSN-5 has been proposed.

2. Materials and methods

2.1. Bacterial and nematode strains, plasmids, and culture conditions

The bacterial strains and plasmids used in this study are listed in Table 1. A wild-type strain of *P. syringae* MB03 [23] (CCTCC No. M2014114, China Center for Type Culture Collection) provided the gene resource for *mcp03*. The *Escherichia coli* strains DH5α, BL21 (DE3), and HT115(DE3) were employed for cloning or expressing certain genes using different plasmid vectors, whereas *E. coli* OP50 cells were used as food for feeding *C. elegans* unless specified. *P. syringae* and *E. coli* cells were routinely cultured at 28 °C and 37 °C in Luria–Bertani (LB) medium [24] supplemented with 100 μg mL^{-1} ampicillin (Amp), 50 μg mL^{-1} kanamycin (Kan), or 20 μg mL^{-1} tetracycline (Tet) when required, respectively. The *C. elegans* strains used in this study include the wild-type Bristol strain N2, green fluorescence protein (GFP)-labeled transgenic strain FT63 (*dlg::gfp*), which were obtained from *Caenorhabditis* Genetics Center (College of Biological Sciences, University of Minnesota, MN55108, USA). The *csn-5* silenced strain was obtained via RNA interference (RNAi) assay. All *C. elegans* strains were cultivated at 25 °C under standard conditions on a nematode growth medium [20] using *E. coli* OP50 as food. The synchronized worms were prepared according to the standard protocol [25].

2.2. Cloning, expression, purification, and labeling of MCP03 protein

The oligonucleotide primers used in this study are listed in Table 1. To construct the recombinant plasmid pMB831 (Fig. 1B), the *mcp03* gene was amplified via polymerase chain reaction (PCR) from the *P. syringae* MB03 genome (GenBank accession No. NZ_LAGV00000000.1) using the primers F-pET28a-mcp03 and R-pET28a-mcp03. The amplified fragment was inserted into the *Xho* I and *Eco*R I sites of the *E. coli* expression vector pET28a to generate pMB831. This recombinant plasmid was subsequently transformed into *E. coli* BL21(DE3) to yield the recombinant strain MB831.

To induce MCP03 expression, *E. coli* MB831 cells were cultured in LB broth with Kan at 37 °C until the cell optical density at 600 nm (OD$_{600}$) reached 0.6, following which 0.2 mmol L^{-1} isopropyl-*β*-ᴅ-thiogalactopyranoside (IPTG) was added to the cultures, which were further incubated at 30 °C for 6 h. The cells were harvested through centrifugation (5000 rpm for 10 min), resuspended in phosphate-buffered saline (PBS, pH 7.4), and homogenized using a high-pressure homogenizer (NS1001L 2 K, Niro Soavi, Germany) at 1000 *psi*. The supernatants were collected through centrifugation (12,000 rpm for 10 min at 4 °C). The MCP03 protein was purified from the supernatants using a nickel nitrilotriacetic acid spin column (Qiagen). The protein samples were subsequently solubilized using 20 mmol L^{-1} HEPES (pH 6.0) and stored at −80 °C following quantification [26]. Finally, the purified MCP03 was labeled using *N*-hydroxysuccinimide-rhodamine (Rho) (Pierce 46,102) [27].

2.3. Nematicidal bioassays

The whole-cell bioassay was performed to identify the nematicidal potential of the MCP03 protein [20]. The expression of the MCP03 protein in the recombinant *E. coli* MB831 cells was induced according to the protocol described in Section 2.2. In each well of a 96-well microtiter plate, 40 μL of recombinant *E. coli* cells with an OD$_{600}$ of 0.7, 5 μL of a worm solution (30–50 worms), 5 μL of 8 mmol L^{-1} FUDR (5-fluorodeoxyuridine), 0.6 μL of 10 mg mL^{-1} chloramphenicol, and S medium were added up to a total volume of 200 μL. The assay plates were then incubated at 25 °C for 5 days. Three replicates were used for each tested sample, and a minimum of three independent experiments were performed. The *E. coli* BL21(DE3) and *P. syringae* MB03 cells were used as negative and positive controls, respectively, in this assay. Experimental nematodes were scored five days after worm deposition and were considered dead when they did not respond to prodding with a platinum wire under a stereomicroscope (Olympus IX73, Tokyo, Japan).

The nematicidal bioassays and the LC$_{50}$ determination of the purified MCP03 protein against *C. elegans* were performed following a previously established method [20]. Briefly, the purified MCP03 sample was tested at different concentrations (45, 90, 135, 180, and 225 μg mL^{-1}). In each well, we added 10 μL of purified MCP03 protein, 5 μL of a worm solution (30–50 worms), 5 μL of 8 mmol L^{-1} FUDR (5-fluorodeoxyuridine), 1 μL of 50 mg mL^{-1} Kan, and S medium supplemented with *E. coli* OP50 as a food source up to a total volume of 200 μL. Each concentration was tested in triplicate, with a minimum of three repetitions. The microtiter plates were sealed

with parafilm to maintain humidity, and the assay was conducted at 25 °C. Furthermore, the death of the worms was recorded after 5 days.

2.4. Growth inhibition and brood size bioassays

The growth inhibition assay was performed using synchronized L1-stage *C. elegans* [20]. Briefly, 10 μL E. *coli* OP50, MCP03 protein at different concentrations (40, 60, 80, 100, and 120 μg mL^{-1}), 1 μL 50 μg mL^{-1} Kanamycin, 5 μL L1 stage larvae of *C. elegans* (30–50 worms), and S medium were added to each well of a 96-well microtiter plate. For a negative control, protein solution was substituted with S medium. Four independent wells and three biological replicates were used for each protein concentration. The worms were consequently incubated for 3 days at 25 °C. First, the nematodes were anesthetized using 15 mmol L^{-1} sodium azide. Then, a minimum of 20 worms were photographed at 100 × magnification using an Olympus digital camera on a microscope (Olympus IX73, Tokyo, Japan) for each concentration. The lengths of these worms were subsequently determined using NIH Image J1.33 software. Finally, we plotted a comparative graph representing the average worm lengths against those of the control group.

The brood size of *C. elegans* was measured in a liquid-based 96-well microtiter plate assay. Each well contained 5 μL E. *coli* OP50 suspension in S medium at an OD$_{600}$ of 0.2, purified MCP03 protein at different concentrations (20, 40, 60, 80, 100, and 120 μg mL^{-1}), a single L4 stage worm, and S medium up to the final volume of 120 μL. Each protein concentration was assayed in four wells with a minimum of three repetitions. Finally, the eggs in each well were counted under an inverted microscope (Olympus IX73, Tokyo, Japan).

2.5. Analysis of C. elegans intestinal pathology

The wild-type *C. elegans* N2 and the transgenic *C. elegans* FT63 (DLG::GFP) were fed with Rho-labeled MCP03 and unlabeled MCP03, respectively. Bovine serum albumin (BSA) was used as the negative control. After 72 h of incubation, the worms were rendered unconscious using a 15 mmol L^{-1} sodium azide and fixed on a microscopic slide coated with 2 % agarose for imaging. The worms were examined using a fluorescence microscope (80i, Nikon, Japan) in two different modes: green fluorescence (GFP) and red fluorescence (RFP).

2.6. Yeast two-hybrid assay

The yeast two-hybrid (Y2H) assays were performed to screen the potential receptor of MCP03 following the standard protocol [28], as shown in Supplementary Fig. S1. A cDNA library from *C. elegans* was constructed using the plasmid vector pGADT7 and transformed into the yeast strain Y187. Full-length MCP03 was fused to the GAL4 DNA binding domain in the vector pGBKT7 to yield the recombinant plasmid pMB832 (Supplementary Fig. S2) and was transformed into the yeast host strain Y2H Gold to yield the recombinant MB832. Two-hybrid interactions were screened by mating MB832 with the A.D. fusion *C. elegans* cDNA library. Blue colonies on SD/-Trp-Leu medium supplemented with X-α Gal (X-alpha galactosidase) and AbA (Aureobasidin A) were further analyzed on SD/-Trp-Leu-His-Ade/X-α Gal/AbA (QDO/X/A) medium. The resultant clones that appeared on the QDO/X/A medium were subjected to colony PCR using specific primers to identify the interacting partners. The resultant *csn-5* was cloned into the vector pGADT7, and the interaction with MCP03 was tested in a Y2H X- α gal assay [28].

2.7. Expression and purification of recombinant protein from C. elegans

Total RNA was extracted from the wild-type strain N2 of *C. elegans* using the Trizol method [29]. Subsequently, cDNA synthesis was performed using the TransScript One-Step gDNA Removal and cDNA Synthesis SuperMix (TransGen Biotech). Furthermore, *csn-5* was amplified using the F-pGEX-6P-1-*csn-5* and R-pGEX-6P-1-*csn-5* primers (Table 1) and then cloned into the expression vector pGEX-6P-1 using the Gibson one-step assembly method [30] to generate the recombinant pMB833 (Supplementary Fig. S3), which was transformed into *E. coli* BL21(DE3) to yield recombinant *E. coli* MB833. For the induction of CSN-5 expression, MB833 cells were cultured in LB broth until an OD$_{600}$ of 0.6 at 37 °C was reached, following which 0.2 mmol L^{-1} IPTG was added, and the cultures were further incubated for 4 h at 30 °C. The recombinant protein was purified using affinity chromatography with glutathione Sepharose 4 B. The eluted protein was subsequently dialyzed and stored at −80 °C.

2.8. Scanning electron microscope

The worm surface morphologies of *C. elegans* N2, MCP03-treated N2, and N2 CSN-5 RNAi were observed under a scanning electron microscope (SEM, JSM-6390/LV, JEOL, Japan) according to the previously described sample preparation and fixation procedures [31].

2.9. Pull-down assay

E. coli MB831 and MB833 expressing His-tag fused MCP03 and glutathione S-transferase (GST) tagged CSN-5, respectively, and *E. coli* MB830 harboring plasmid pGEX-6P-1 (as the negative control) were IPTG-induced according to the above protocols. The cells were harvested via centrifugation at 12,000 rpm for 10 min at 4 °C, resuspended with PBS (pH 7.4), and homogenized using a high-

pressure homogenizer (NS1001L 2 K, Niro Soavi, Germany) at 1000 *psi*. Following centrifugation of the disrupted suspensions, the supernatants from MB831/MB833 and MB831/MB830 (the negative control) were grouped and incubated with glutathione-coupled Sepharose beads in a rotative incubator for 3 h at 4 °C, following which they were centrifuged. The beads were washed with precooled (4 °C) PBS (pH 7.4) at least five times to elute unbound proteins. The bead-bound proteins were detected using 12.5 % sodium dodecyl sulfate–polyacrylamide gel electrophoresis (SDS–PAGE) and Western blot analysis using an anti-His-tag antibody, according to the standard protocols [24].

2.10. Western blot analysis

To analyze the expression of MCP03 in *E. coli* MB831 and the binding interaction between MCP03 and CSN-5, after the separation of total proteins via 10 % and 12.5 % SDS–PAGE, respectively, the gels were electro-transferred to a nitrocellulose membrane and incubated overnight with a 1:11,000 dilution of anti-His-tag antibody, followed by incubation with an HRP-conjugated secondary antibody at a 1:1500 dilution. The membrane was then visualized using an enhanced chemiluminescence substrate as described by the manufacturer (Bio-Rad Laboratories, Inc., Hercules, CA, USA).

2.11. Construction of csn-5 RNAi strain

An RNAi strain (namely *E. coli* MB834) was constructed and used to silence *csn-5* expression in *C. elegans* N2 following a previously described protocol [32]. The *csn-5* fragment was PCR-amplified from the cDNA of *C. elegans* N2 using the primers F-RNAi.*csn*-5 and R-RNAi.*csn*-5 (Table 1). The amplified fragment was subsequently digested using *Hin*d III and cloned into an RNAi plasmid vector pL4440 to yield recombinant pMB834 (Supplementary Fig. S4A), which was transformed into *E. coli* HT115 to generate *E. coli* MB834. The expression of dsRNA in MB834 was induced using 1 mmol L^{-1} IPTG at the final concentration (Supplementary Fig. S4B).

2.12. Real-time quantitative PCR

Synchronized *C. elegans* N2 L4 stage worms were fed with purified MCP03 or BSA (negative control). The worms were collected 24 h after feeding and used for extracting total RNAs according to a previously reported protocol [29]. Real-time quantitative PCR (RT-qPCR) was performed to determine the expression levels of selected *C. elegans* genes using the comparative cycle threshold method ($2^{-\triangle\triangle C.T.}$ method) [33]. The primers used for RT-qPCR analysis of the selected genes are listed in Table 1. *GAPDH* was used as an internal reference gene, while RNAs from BSA-fed *C. elegans* N2 were used as the negative control.

2.13. Data analysis

Statistical analysis was performed using GraphPad Prism 8.3 (GraphPad Software, LLC, Boston, MA, USA), and data were derived from at least three biological replicates unless otherwise indicated. Statistical significance was defined as $p < 0.05$.

3. Results

3.1. Molecular characterization, expression and purification, and nematicidal activity of MCP03

The gene *mcp03* (gene locus *"VT47_10,710"*) from the genome of *P. syringae* MB03 was characterized using the online tool BLASTn in the GenBank nucleotide sequence database at the National Center for Biotechnology Information server (https://blast.ncbi.nlm.nih.gov/Blast.cgi). The MCP03 protein was predicted to encode a 598 amino acid (AA) protein with a theoretical molecular weight (Mw) of ~66 kDa. Conserved domain architecture analysis revealed two domains of MCP03: a HAMP domain, spanning AAs 93–149, and an MCP signal domain, spanning AAs 154–424 (Fig. 1A). The gene *mcp03* was amplified from the *P. syringae* MB03 genome and was expressed in *E. coli* MB831 via constructing an expression plasmid pMB831 (Fig. 1B). Fig. 1C shows that an additional band with a molecular mass equal to that of the predicted MCP03 was present in the *E. coli* MB831 profile (indicated by the arrow). However, this was not found in the BL21(DE3) profile (the negative control), indicating the successful expression of MCP03 in *E. coli* MB831 cells. Subsequently, a liquid-based bioassay was performed to evaluate the virulence potential of *E. coli* MB831 intact cells toward *C. elegans*. MB831 exhibited significant ($p < 0.001$) nematicidal activity against *C. elegans* compared with that shown by the negative control *E. coli* BL21(DE3) cells (*P. syringae* MB03 intact cells were used as a positive control) (Fig. 1D). Therefore, the MCP03 protein expressed in MB831 was purified, and SDS–PAGE and Western blot analyses confirmed that MCP03 was purified as a single protein component at high purity (Fig. 1E & F). We further evaluated the nematicidal activity of the purified MCP03 against *C. elegans*. Fig. 1G shows that the purified MCP03 exhibited pronounced nematicidal activity against *C. elegans* in a dose-dependent pattern, with a calculated LC_{50} value of 124.47 (99.22–147.47) μg mL^{-1}, indicating the high toxicity of this protein against *C. elegans*.

3.2. MCP03 affects different phenotypes of C. elegans

The virulence of purified MCP03 protein was assessed by investigating its effects on the spawning number and growth of *C. elegans* N2, using BSA as the negative control. Fig. 2A shows the detrimental effect of MCP03 on the brood size of worms following a dose increase from 0 to 120 μg mL^{-1}, and the spawning rate declined to 0 at a dose of 120 μg mL^{-1}, indicating the pathogen-induced

impairment of the reproductive system of *C. elegans* N2 when fed MCP03. Moreover, Fig. 2B shows that low MCP03 concentrations (<20 µg mL^{-1}) exerted only a slight repressive effect on the size of the synchronized L1-stage *C. elegans* worms; however, higher MCP03 concentrations induced a greater decrease in worm size, and at 120 µg mL^{-1} of MCP03, the area of the worm was only 20 % compared to the control BSA, thereby indicating a dose-dependent detrimental effect of MCP03 on the growth of *C. elegans*.

Interestingly, MCP03 also demonstrated disruptive impairment on the surface cuticles of *C. elegans* N2, as severe depressed dents and wrinkles of the cuticles were clearly visualized under SEM on the surface phenotype of worms fed with MCP03 in 72 h, which strongly contrasted with the smooth surface of worms fed with BSA (Fig. 2C).

To investigate whether MCP03 acted on the intestinal tract of worms, we examined the intestinal morphology of two *C. elegans* worms that were fed with Rho-labeled or un-labeled MCP03 after 72 h: the wild-type N2 and GFP-tagged FT63 (*dlg::gfp*) respectively. Fig. 2D shows that the intestinal tract of N2 treated with Rho-labeled MCP03 appeared to be pathologically altered under the upper CLSM micrography, as disseminative red fluorescence was distributed throughout the entire worm body, while the control N2 fed with Rho-labeled BSA displayed red fluorescence confined to only the intestinal tract. Moreover, the destructive effect of MCP03 on the integrity of the epithelial junctions of worms was confirmed using MCP03-treated FT63(*dlg::gfp*) worms as substantial disruption of epithelial junctions was visible via upper CLSM micrography (Fig. 2E) (indicated by the yellow dotted–rectangle region). Conversely, the control worm fed with BSA exhibited an integrated, intact, bamboo-shaped intestinal tract.

3.3. Identification of CSN-5 as a putative receptor of MCP03

To identify the receptor protein interacting with MCP03 to approximately actuate its toxicity against *C. elegans* N2, we performed an N2 genome-wide Y2H screening using MCP03 as the bait. We first performed the control experiments; the positive controls, pGBKT7-53 and pGADT7-T, exhibited interaction on the DDO/X/A plate (Supplementary Fig. S5A), validating the assay's sensitivity. Meanwhile, the negative control, involving pGADT7-T and pGBKT7-Lam, demonstrated the absence of interaction, confirmed by the
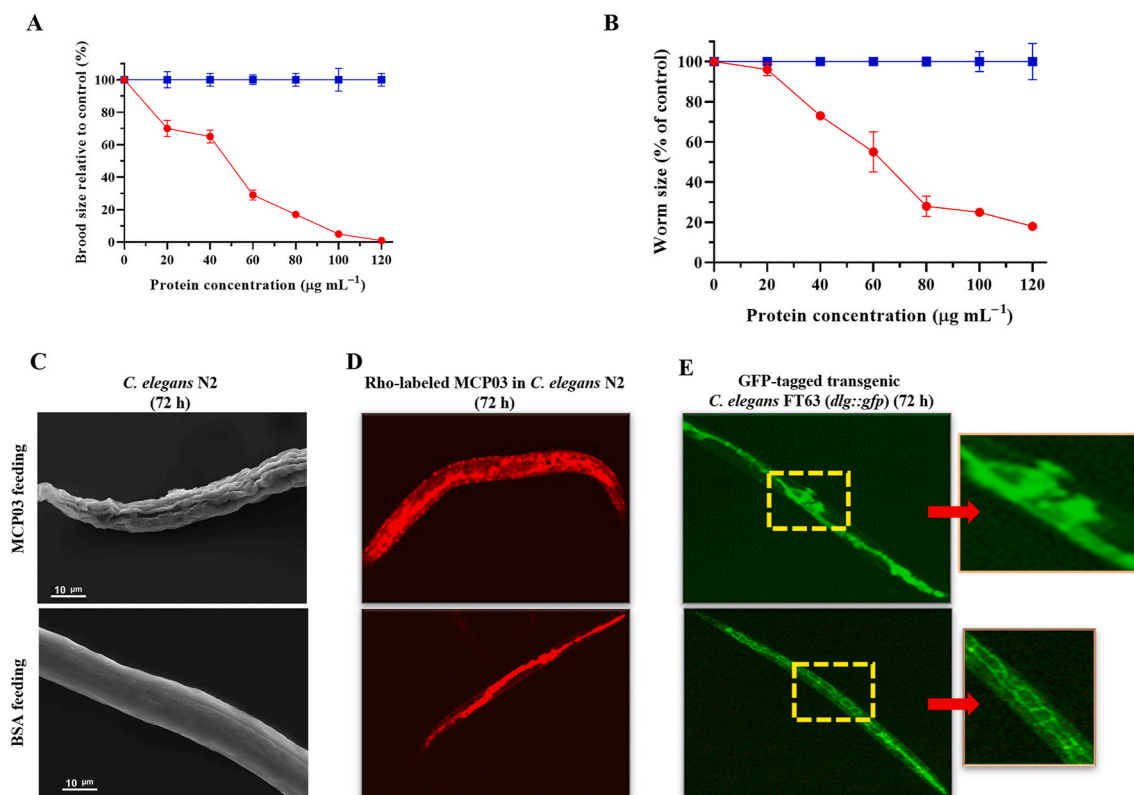

Fig. 2. Detrimental effects of MCP03 on *C. elegans* N2. (**A**) Brood size assay of *C. elegans* under different concentrations of MCP03. (**B**) Worm size assay of *C. elegans* treated with different doses of MCP03. (**C**) SEM micrograph of the surface morphology of *C. elegans* after feeding with MCP03 or BSA. (**D**) Fluorescence micrograph of *C. elegans* N2 fed with Rho-labeled MCP03 (Magnification: 400×). Rho-labeled BSA was used as the negative control. In the MCP03-treated worm, red fluorescence was distributed throughout the entire body, while the control N2 fed with Rho-labeled BSA displayed red fluorescence confined to only the intestinal tract. (**E**) Fluorescence micrograph of GFP-tagged *C. elegans* FT63 (*dlg::gfp*) fed with MCP03 (Magnification: 400×). The yellow-dotted rectangle in the treated nematode micrograph highlights the area of intestinal tissue damage, indicating blurry and fragmented GFP fluorescence. Conversely, the intestine of the control worm fed with BSA exhibited an integrated, intact bamboo-shaped intestinal tract. (For interpretation of the references to colour in this figure legend, the reader is referred to the Web version of this article.)

lack of growth on the DDO/X/A plate (Supplementary Fig. S5B). Fig. 3A shows a typical trilobite pattern of mating yeast cells, indicating the successful mating of MB832 and the Y187 Y2H library cells carrying various fractions of *C. elegans* cDNA. Fig. 3B shows blue colonies on QDO/X/A plates, indicating the presence of potential prey proteins interacting with MCP03 in these colonies. Therefore, these four colonies were subjected to PCR amplification of their harbored prey cDNAs, revealing that all four prey cDNA fragments were of similar size in the electrophoresis profiles (~1100 bps) (Fig. 3C). These fragments were sequenced and found to be an identical ORF comprising 1107-bp nucleotide sequences, which was further identified as the *csn-5* gene of *C. elegans* by searching the WormBase database (https://wormbase.org//). CSN-5 was the exclusive candidate receptor in our yeast two-hybrid screen, signifying a specific and substantial interaction within our experimental framework. Notably, the limited number of hits may result from variations in screening conditions or bait selection. The predicted protein CSN-5 comprises 369 AA with a theoretical Mw of ~67 kDa and is a key subunit of the COP9 signalosome. This conserved protein complex plays a critical role in regulating gene expression, cell proliferation, and eukaryotic cell cycle [34]. Conserved domain architecture analysis revealed that CSN-5 possesses an MPN superfamily domain spanning AA45–AA292. Three motifs within this domain were identified, namely Mov34/MPN/JAMM, as well as a zinc-binding site with metalloproteinase activity (Supplementary Fig. S6A). The three-dimensional structure of CSN-5 exhibits a compact architecture characterized by multiple α-helices and β-sheets that form a barrel fold (Supplementary Fig. S6B).

3.4. Binding interaction of MCP03 with CSN-5

An in vivo yeast response validation of CSN-5 via the cotransformation of bait plasmid pMB832 and prey plasmid pGADT7-*csn-5* into Y187 revealed a positive colony of CSN-5 (Fig. 3D), thereby verifying the binding between CSN-5 and MCP03. *In vitro,* pull-down affinity chromatography assay and Western blot analysis were also performed to confirm the binding activity of the purified GST-tagged CSN-5 protein (GST–CSN-5) and MCP03. Fig. 4A shows that GST–CSN-5 was successfully expressed in *E. coli* MB833, with the predicted Mw of ~67 kDa (Fig. 4A, lane 2 indicated by blue arrow), while His-tagged MCP03 was expressed in MB831 at the Mw of ~66 kDa (Fig. 4A, lane 3 indicated by red arrow). Following coincubation of the purified GST–CSN-5 and MCP03, they formed a binding complex that was identified in the SDS–PAGE profile (Fig. 4A, lane 5). Conversely, no binding complex was detected in the coincubation of GST and MCP03 alone (Fig. 4A, lane 4). Western blot analysis using a specific anti-His antibody further visualized a ~67 kDa positive band in the GST–CSN-5/MCP03 complex, slightly higher than that of the control MCP03 at ~66 kDa, which appeared to be caused by the complex formed with GST–CSN-5 at a relatively higher Mw (Fig. 4B). Overall, these results confirm the binding activity between MCP03 and CSN-5.

3.5. Effects of silencing csn-5 by RNAi on brood size, growth size, and cuticle integrity

RNAi experiments were conducted to silence *csn-5* in *C. elegans* N2 (the RNAi-treated *C. elegans* N2 was named "N2-CSN-5-RNAi"). The growth, brood size, and cuticle morphology of N2-CSN-5-RNAi were then compared with N2. The *csn-5* gene of N2 was cloned to pL4440 to construct pMB834, and a 1273-bp dsRNA specific for *csn-5* RNAi was synthesized upon IPTG induction in *E. coli* MB834 cells harboring pMB834 (Supplementary Fig. S4A). The *C. elegans* N2-CSN-5-RNAi worms were yielded by feeding the dsRNA to N2. Fig. 5 shows only a limited effect of *csn-5* RNAi on the growth of N2 (Fig. 5A) and the average individual size of twenty worms (Fig. 5B), indicating that CSN-5 did not significantly regulate the growth of *C. elegans* ($p > 0.05$). However, the RNAi on *csn-5* caused a significant inhibitory effect on the brood size of N2-CSN-5-RNAi compared to N2, as the N2-CSN-5-RNAi worms laid approximately 65 % fewer eggs compared with that of the wild-type N2 ($p < 0.05$) (Fig. 5C), indicating that CSN-5 served as the action receptor of MCP03 in suppressing the reproduction system of *C. elegans*. Moreover, the *csn-5* RNAi caused morphological changes on the surface cuticles of worms, as the crumples and depressed dents of the cuticles were visible in the N2-CSN-5 RNAi worms (Fig. 5D, indicated by the red
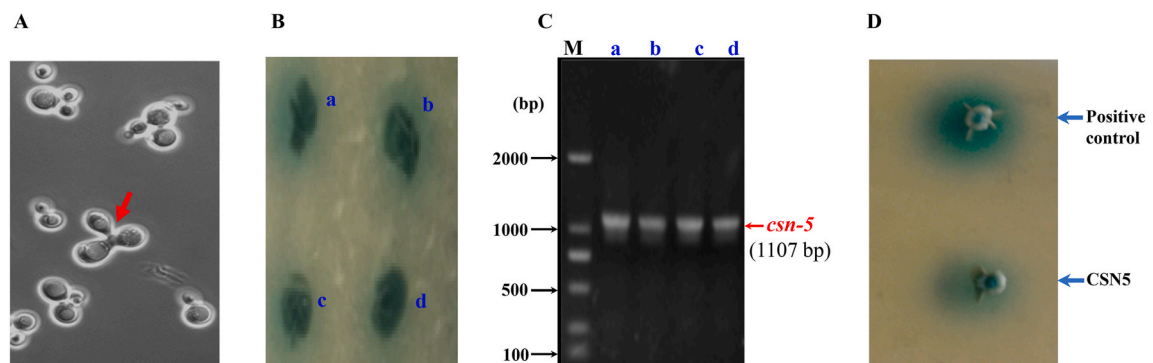

Fig. 3. Yeast two-hybrid assay for the identification of the MCP03-interacting receptor. (**A**) Micrograph of the mating yeast cells. The red arrow indicates a typically successful trilobite mating pattern. In (**B**), (a)–(d) indicate positive colonies in the preliminary screening on the QDO/X/A medium plate. (**C**) Electrophoresis of PCR-amplified plasmid cDNAs from positive colonies. Lane M, DNA Mw marker. Lane (a)–(d), PCR-amplified products from the colony a–d on (**B**). (**D**) Yeast response validation on CSN-5 by cotransformation of bait plasmid pMB832 and prey plasmid pGADT7-*csn-5* into Y187. (For interpretation of the references to colour in this figure legend, the reader is referred to the Web version of this article.)
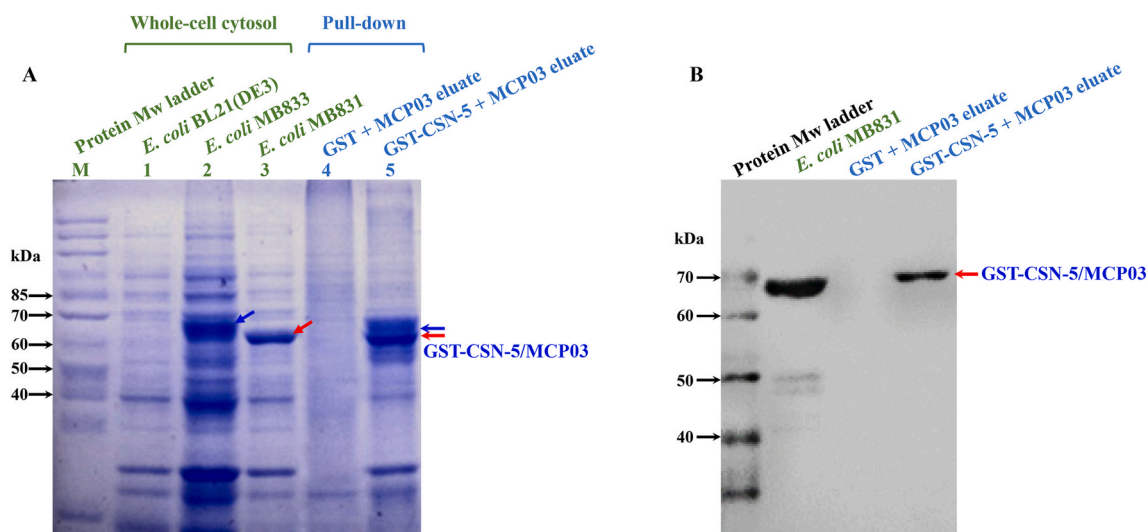
Fig. 4. Binding interaction between MCP03 and CSN-5. (**A**) SDS–PAGE analysis of recombinant *E. coli* cells expressing CSN-5 and *in vitro* pull-down assay of MCP03 and CSN-5 interaction. (**B**) Western blot analysis of the pull-down fractions.

arrow), consistent with the similar pathological pattern of MCP03 treatment (Fig. 5D), further identifying that CSN-5 is a functional action receptor of MCP03.

3.6. RT-qPCR analysis of selected genes of C. elegans N2

To investigate the effects of MCP03 on *C. elegans* at the molecular level, we conducted RT-qPCR analysis on a subset of genes associated with growth, brood size, and cuticle formation of the worm. Specifically, we analyzed the expression levels of *col-117*, which encodes collagen belonging to the Col-3 family and serves as the main component of stratum corneum on the *C. elegans* surface [35], *kgb-1*, a gene involved in regulating the reproductive function of *C. elegans* [36], *unc-98*, a gene involved in the assembly and maintenance of myofibrils [37,38], and *mpk-1*, a gene involved in regulating the resveratrol-mediated longevity of *C. elegans* through MPK-1 signaling pathways [39]. Fig. 6 shows that after feeding MCP03 for 24 h, the expression levels of *col-117*, *kgb-1*, and *unc-98* in *C. elegans* N2 were substantially downregulated, those of *mpk-1* were significantly upregulated, and those of *csn-5* remained unchanged. The downregulation of *col-117* expression is consistent with the observed depressed morphology of stratum corneum on the worm surface after feeding MCP03 (Fig. 5D); the downregulation of *kgb-1* affected the fertility of worms, as identified previously because KGB-1 and CSN-5 interact with GLH-1 and regulate the reproductive function of nematodes [38]. In addition, the downregulation of *unc-98* affected the formation of *C. elegans* muscle tissue [40]. These results suggest that MCP03 has a significant impact on the expression levels of key genes associated with *C. elegans* cuticle formation, reproduction, growth, and muscle tissue development, elucidating the molecular mechanisms underlying its effects on these physiological processes.

4. Discussion

This study aimed to investigate the nematicidal activity and underlying action mechanism of MCP03 in the *P. syringae* MB03-*C. elegans* infection model. We evaluated the direct nematicidal activity of MCP03 against *C. elegans* and its detrimental effects on the growth, brood size, and external and internal morphology of *C. elegans*. Furthermore, we identified CSN-5 as an MCP03-binding protein in *C. elegans*. Although the role of MCPs as key players in chemotaxis and pathogenicity has been well-characterized in different bacteria [41], to the best of our knowledge, this study was the first to provide new insights into the nematicidal activity and action mechanism of a bacterial MCP against nematodes.

In the *P. syringae* MB03 genome, 46 MCP-encoding genes (chemoreceptor genes) were annotated. Notably, the genome-wide prediction of nematicidal genes of *P. syringae* MB03 using VirulentPred and a liquid fast-killing assay using recombinant *E. coli* cells revealed the nematicidal potential of MCP03 among these MCPs [21]. Consistent with this prediction, the bioassays of heterologously expressed MCP03 exhibited lethal activity against *C. elegans*, with an LC$_{50}$ of 124.47 (99.22–147.47) µg mL^{-1}, and multiple detrimental effects on the growth, reproduction, and morphology of *C. elegans*. Although the activity is relatively lower than that of Cry5Da1, a well-known eminent bacterial nematicidal toxin of *B. thuringiensis* with an LC$_{50}$ of 36.69 µg mL^{-1} against *C. elegans* [42], given the multifaceted nematode-toxic activities, MCP03 still holds promise as a potential nematode-pest control agent for agricultural, horticultural, or forestry applications.

CSN-5 is a gene in *C. elegans* that encodes a component of the COP9 signalosome (CSN) complex. *C. elegans* contains seven CSN subunits (CSN 1, 2, 3, 4, 5, 6, and 7), which possess proteasome component domains that promote protein–protein interactions and have nucleic acid–binding properties [43]. Conversely, CSN-5 and CSN-6 possess an MPN domain with a JAMM (Jab/MPN/Mov34)
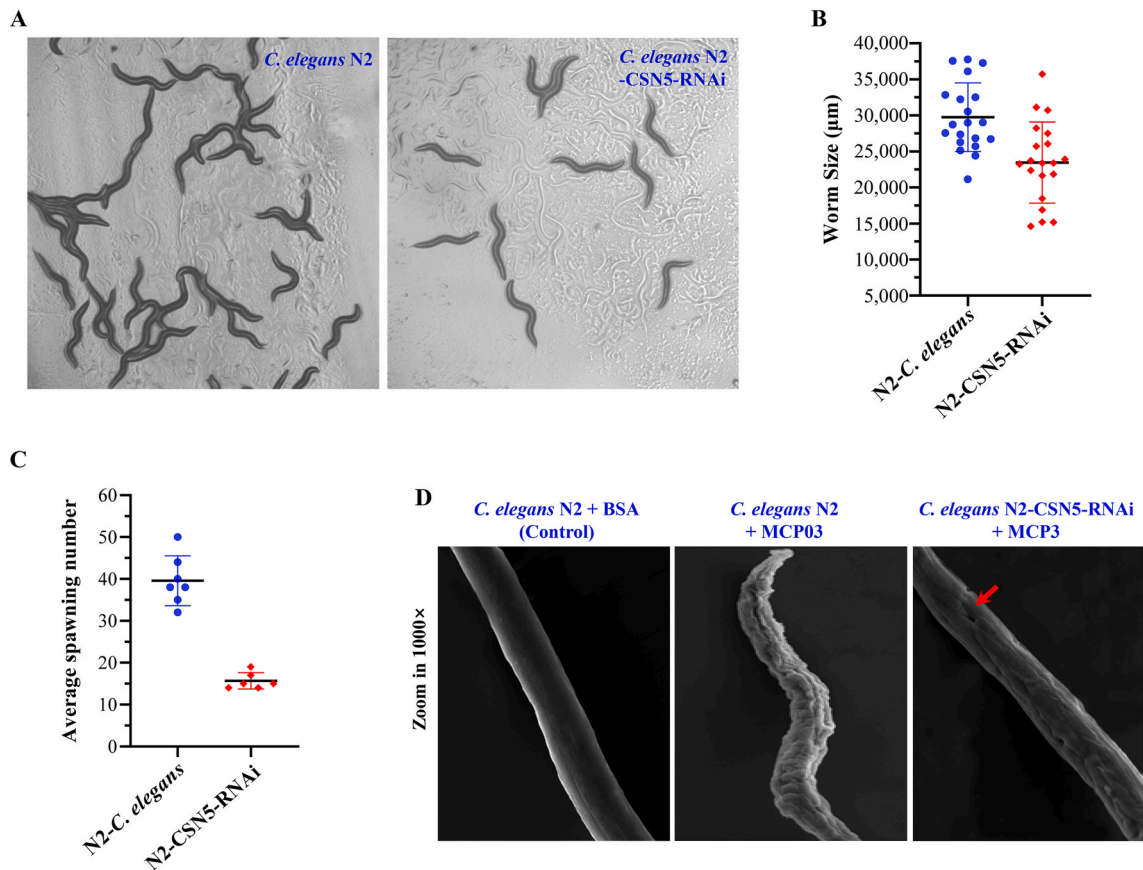
Fig. 5. Effects of *csn-5* RNAi on the worm size, brood size, and surface cuticle of *C. elegans* N2. (**A**) Microscopic examination of the wild-type and *csn-5* RNAi-treated *C. elegans* N2 worms (Magnification: 40×). (**B**) Worm size quantification of the wild-type and *csn-5* RNAi-treated *C. elegans*. CSN-5 did not significantly ($p > 0.05$) regulate the growth of *C. elegans*. (**C**) Quantification of the average spawning number of the wild-type and *csn-5* RNAi-treated *C. elegans*. CSN-5 caused a significant ($p < 0.05$) inhibitory effect on the brood size of N2-CSN-5-RNAi compared to N2. (**D**) SEM micrograph of the *csn-5* RNAi-*C. elegans* worms. The wild-type N2 worms fed with BSA and MCP03 were used as the negative and positive controls, respectively. The red arrow indicates the depressed dent of the worm surface. (For interpretation of the references to colour in this figure legend, the reader is referred to the Web version of this article.)

sequence and exhibit metalloproteinase activity [44]. The three-dimensional structure of CSN-5 exhibits a compact architecture characterized by multiple α-helices and β-sheets that form a barrel fold responsible for mediating protein–protein interactions (Supplementary Fig. S6B) [45]. Notably, CSN-5 is also involved in ubiquitin-dependent protein degradation, cell cycle regulation, and multiple signal transduction processes [46]. This suggests its potential role in mediating crucial protein–protein interactions central to these cellular functions. Herein, CSN-5 was identified as the binding receptor of MCP03 through two distinct *in vitro* experiments. Owing to the unavailability of the CSN-5:GFP strain of *C. elegans*, we were unable to identify the in vivo interaction between MCP03 and CSN-5 proteins in this study as constructing such a strain was not feasible within the constraints of our laboratory resources and it was also not available through CGC. The data shown in Fig. 2 indicate that MCP03 targeted the intestinal tissues of N2 and caused severe destructive impairment of the integrity of epithelial junctions. We believe that these pathological changes could be the main lethal determinants of MCP03 treatment as these changes are associated with other stepwise pathological processes, such as decreased food intake, substance, and energy metabolism collapse, and septicemia, which ultimately lead to the death of *C. elegans*. Evaluating the impact of MCP03 treatment on *C. elegans* intestinal permeability at sequential time points would provide valuable insights into anatomical changes of the intestine in correlation with variations in worm size. However, whether these pathological processes were related to the binding of MCP03 and CSN-5 remains unknown. Therefore, further studies are warranted to include the expression of CSN5 in RNAi knockdown *C. elegans* to demonstrate if the nematicidal activity of MCP03 is restored. Additionally, the changes in the structure and permeability of the intestines after the suppression of CSN5 could be tested to explore the role and action mechanism of the MCP03-CSN-5 binding complex in the pathogenicity of MCP03.

Several investigations have demonstrated that CSN-5 interacts with UNC-98 and UNC-96, which are involved in the assembly and maintenance of myofibers [37]. The outer surface of MCP03-treated N2 severely shrank (Fig. 2C), *col-117* and *unc-98* expressions were significantly downregulated (Fig. 6), and the cuticle of worms subjected to CSN-5 RNAi silencing exhibits a pathological pattern consistent with the effects observed in worms treated with MCP03 (Fig. 5D). These results suggest that MCP03 interacts with CSN-5
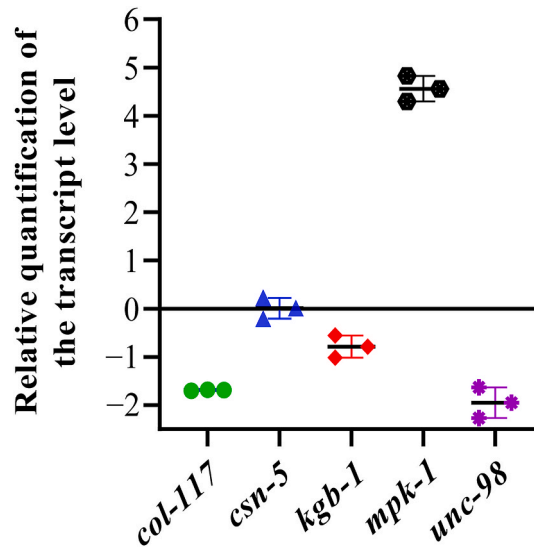
Fig. 6. RT-qPCR of expression activities of several selected genes related to fertility, growth, and cuticle formation of *C. elegans*.

and downregulates the expression of collagen and certain muscle-related proteins, causing severely depressed wrinkles on the surface of the worms. In addition, Fig. 2A illustrates that MCP03 had a substantial inhibitory effect on the reproductive capacity of N2, leading to a significant reduction in brood size. RNAi with *csn-5* significantly reduced the spawning rate of N2 (Fig. 5C), confirming the critical role of CSN-5 in regulating the fertility activity of *C. elegans*. This could be attributed to the downregulation of *kgb-1* expression, as CSN-5 and KGB-1 can regulate the expression of GLH-1, which is crucial for the fertility of *C. elegans* [36]. Notably, the expression of *csn-5* in N2 remained unaltered following MCP03 treatment. We speculate that MCP03 was bound to CSN-5 and inhibited its activity to some extent without significantly reducing the expression of the protein. However, MCP03 may interact with other undetected receptors in *C. elegans*, potentially because of limitations in the coverage of the cDNA library and screening processes employed in this study.

Based on the results obtained in this study, we propose a few outlines for the pathogenicity of MCP03 against *C. elegans* (Fig. 7). When MCP03 infects *C. elegans* worms, it impacts their epidermal layer, reducing collagen expression and deteriorating the stratum corneum. DAF-16 is positively regulated when worms are infected, and the epidermis is damaged [47]. Consequently, the nematodes detect external threats, which trigger their immune response and upregulate the expression of MPK-1, which promotes resveratrol-mediated nematode lifespan in a non-dependent manner through the SIR-2.1/DAF-16 pathway (closely related to regulating nematode lifespan and immunity) by regulating SKN-1 accumulation in the nucleus [39]. Furthermore, MCP03 interacts with CSN-5 gene within the nematode, which exerts an inhibitory effect on CSN-5 activity, which subsequently impacts various aspects of nematode physiology, notably the fertility-related gene *glh*-1 that interacts with CSN-5 and the *unc-98* and *unc-96* genes that are associated with myofibril function. Consequently, the egg-laying rate of nematodes decreases, and their outer surface undergoes shrinkage. It is important to highlight the involvement of CSN-5 within nematodes in mediating ubiquitin-dependent protein degradation. Cellular protein degradation predominantly relies on the ubiquitin–proteasome system. The disruption of this system can result in severe consequences, including cell cancer or necrosis. After feeding on MCP03, nematodes also experience certain intestinal damage, which may be linked to the CSN-5 receptor protein. However, the precise underlying mechanisms of this intestinal damage warrant further research for a comprehensive understanding.

5. Conclusions

The present study demonstrates the nematicidal activity of MCP03 against *C. elegans* and the detrimental effects on intestinal tissues, fertility capability, growth, and surface cuticle morphology. Y2H assays identified a subunit of the CSN signaling complex, CSN-5, as an action receptor of MCP03. The binding interaction between MCP03 and CSN-5 was confirmed through two distinct *in vitro* experiments such as Yeast two-hybrid and pull-down assays. Following the MCP03 treatment, several genes related to fertility, growth, and cuticle formation were found to be downregulated in N2 worms. Owing to its relatively high nematicidal virulence and multiple detrimental activities, MCP03 has the potential to be pursued for developing a bionematicide.

Data availability statement
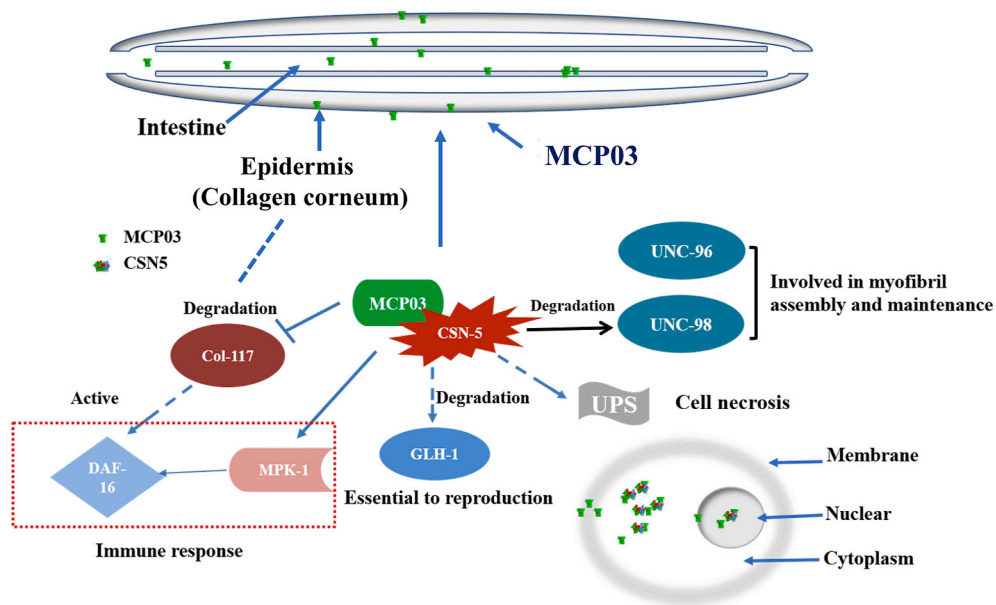
Data will be made available upon request.

Fig. 7. The proposed action mechanism underlying MCP03 pathogenicity against *C. elegans*.

CRediT authorship contribution statement

Jiaoqing Li: Writing – original draft, Validation, Methodology, Investigation, Funding acquisition, Data curation, Conceptualization. **Haiyan Dai:** Writing – original draft, Validation, Methodology, Investigation, Formal analysis, Data curation. **Anum Bashir:** Writing – original draft, Methodology, Investigation, Formal analysis, Data curation. **Zhiyong Wang:** Methodology, Investigation. **Yimin An:** Formal analysis, Data curation. **Xun Yu:** Writing – review & editing, Investigation. **Liangzheng Xu:** Supervision, Conceptualization. **Lin Li:** Writing – review & editing, Supervision, Funding acquisition, Data curation, Conceptualization.

Declaration of competing interest

The authors declare no competing financial interests.

Acknowledgments

Appendix B. Supplementary data

Supplementary data to this article can be found online at https://doi.org/10.1016/j.heliyon.2024.e30366.

References

[1] P. Abad, J. Gouzy, J.M. Aury, P. Castagnone-Sereno, E.G.J. Danchin, E. Deleury, L. Perfus-Barbeoch, V. Anthouard, F. Artiguenave, V.C. Blok, M.C. Caillaud, P. M. Coutinho, C. Dasilva, F. De Luca, F. Deau, M. Esquibet, T. Flutre, J.V. Goldstone, N. Hamamouch, T. Hewezi, O. Jaillon, C. Jubin, P. Leonetti, M. Magliano, T. R. Maier, G.V. Markov, P. McVeigh, G. Pesole, J. Poulain, M. Robinson-Rechavi, E. Sallet, B. Ségurens, D. Steinbach, T. Tytgat, E. Ugarte, C. van Ghelder, P. Veronico, T.J. Baum, M. Blaxter, T. Bleve-Zacheo, E.L. Davis, J.J. Ewbank, B. Favery, E. Grenier, B. Henrissat, J.T. Jones, V. Laudet, A.G. Maule, H. Quesneville, M.N. Rosso, T. Schiex, G. Smant, J. Weissenbach, P. Wincker, Genome sequence of the metazoan plant-parasitic nematode *Meloidogyne incognita*, Nat. Biotechnol. 26 (2017) 909–915, https://doi.org/10.1038/nbt.1482.
[2] O. Topalović, S. Geisen, Nematodes as suppressors and facilitators of plant performance, New Phytol. 238 (2023) 2305–2312, https://doi.org/10.1111/nph.18925.
[3] P. Castillo, J.A. Navas-Cortés, B.B. Landa, R.M. Jiménez-Díaz, N. Vovlas, Plant-parasitic nematodes attacking chickpea and their in planta interactions with rhizobia and phytopathogenic fungi, Plant Dis. 92 (2008) 840–853, https://doi.org/10.1094/PDIS-92-6-0840.

[4] R. Sabbahi, V. Hock, K. Azzaoui, S. Saoiabi, B. Hammouti, A global perspective of entomopathogens as microbial biocontrol agents of insect pests, J. Agric. Food Res. 10 (2022) 100376, https://doi.org/10.1016/j.jafr.2022.100376.

[5] H. Luo, J. Xiong, Q. Zhou, L. Xia, Z. Yu, The effects of *Bacillus thuringiensis* Cry6A on the survival, growth, reproduction, locomotion, and behavioral response of *Caenorhabditis elegans*, Appl. Microbiol. Biotechnol. 97 (2013) 10135–10142, https://doi.org/10.1007/s00253-013-5249-3.

[6] D. Peng, J. Lin, Q. Huang, W. Zheng, G. Liu, J. Zheng, L. Zhu, M. Sun, A novel metalloproteinase virulence factor is involved in *Bacillus thuringiensis* pathogenesis in nematodes and insects, Environ. Microbiol. 18 (2016) 846–862, https://doi.org/10.1111/1462-2920.13069.

[7] J.F. Dubern, C. Cigana, M. De Simone, J. Lazenby, M. Juhas, S. Schwager, I. Bianconi, G. Döring, L. Eberl, P. Williams, A. Bragonzi, M. Cámara, Integrated whole-genome screening for *Pseudomonas aeruginosa* virulence genes using multiple disease models reveals that pathogenicity is host specific, Environ. Microbiol. 17 (2015) 4379–4393, https://doi.org/10.1111/1462-2920.12863.

[8] X. Sun, R. Zhang, M. Ding, Y. Liu, L. Li, Biocontrol of the root-knot nematode *Meloidogyne incognita* by a nematicidal bacterium *Pseudomonas simiae* MB751 with cyclic dipeptide, Pest Manag. Sci. 77 (2021) 4365–4374, https://doi.org/10.1002/ps.6470.

[9] V. Phani, T.N. Shivakumara, K.G. Davies, U. Rao, *Meloidogyne incognita* fatty acid- and retinol-binding protein (Mi-FAR-1) affects nematode infection of plant roots and the attachment of *Pasteuria penetrans* endospores, Front. Microbiol. 8 (2017) 2122, https://doi.org/10.3389/fmicb.2017.02122.

[10] P. Tedesco, E. Di Schiavi, F.P. Esposito, D. de Pascale, Evaluation of *Burkholderia cepacia* complex bacteria pathogenicity using *Caenorhabditis elegans*, Bio. Protoc. 6 (2016) e1964, https://doi.org/10.21769/BioProtoc.1964.

[11] X. Huang, B. Tian, Q. Niu, J. Yang, L. Zhang, K. Zhang, An extracellular protease from *Brevibacillus laterosporus* G4 without parasporal crystals can serve as a pathogenic factor in infection of nematodes, Res. Microbiol. 156 (2005) 719–727, https://doi.org/10.1016/j.resmic.2005.02.006.

[12] N. Crickmore, Using worms to better understand how *Bacillus thuringiensis* kills insects, Trends Microbiol. 13 (2005) 347–350, https://doi.org/10.1016/j.tim.2005.06.002.

[13] G.H. Wadhams, J.P. Armitage, Making sense of it all: bacterial chemotaxis, Nat. Rev. Mol. Cell Biol. 5 (2004) 1024–1037, https://doi.org/10.1038/nrm1524.

[14] S. Nishiyama, D. Suzuki, Y. Itoh, K. Suzuki, H. Tajima, A. Hyakutake, M. Homma, S.M. Butler-Wu, A. Camilli, I. Kawagishi, Mlp24 (McpX) of *Vibrio cholerae* implicated in pathogenicity functions as a chemoreceptor for multiple amino acids, Infect. Immun. 80 (2012) 3170–3178, https://doi.org/10.1128/IAI.00039-12.

[15] Y. Choi, S. Kim, H. Hwang, K.P. Kim, D.H. Kang, S. Ryu, Plasmid-encoded MCP is involved in virulence, motility, and biofilm formation of *Cronobacter sakazakii* ATCC 29544, Infect. Immun. 83 (2015) 197–204, https://doi.org/10.1128/IAI.02633-14.

[16] H.P. McLaughlin, D.L. Caly, Y. McCarthy, R.P. Ryan, J.M. Dow, An orphan chemotaxis sensor regulates virulence and antibiotic tolerance in the human pathogen *Pseudomonas aeruginosa*, PLoS One 7 (2012) e42205, https://doi.org/10.1371/journal.pone.0042205.

[17] X. Yu, S.P. Lund, R.A. Scott, J.W. Greenwald, A.H. Records, D. Nettleton, S.E. Lindow, D.C. Gross, G.A. Beattie, Transcriptional responses of *Pseudomonas syringae* to growth in epiphytic versus apoplastic leaf sites, Proc. Natl. Acad. Sci. U.S.A. 110 (2013) E425–E434, https://doi.org/10.1073/pnas.1221892110.

[18] M.A. Matilla, T. Krell, The effect of bacterial chemotaxis on host infection and pathogenicity, FEMS Microbiol. Rev. 42 (2018), https://doi.org/10.1093/femsre/fux052.

[19] M. Ali, Y. Sun, L. Xie, H. Yu, A. Bashir, L. Li, The pathogenicity of *Pseudomonas syringae* MB03 against *Caenorhabditis elegans* and the transcriptional response of nematicidal genes upon different nutritional conditions, Front. Microbiol. 7 (2016) 805, https://doi.org/10.3389/fmicb.2016.00805.

[20] A. Bashir, Y. Sun, X. Yu, X. Sun, L. Li, Nematicidal effects of 2-methyl-aconitate isomerase from the phytopathogen *Pseudomonas syringae* MB03 on the model nematode *Caenorhabditis elegans*, J. Invertebr. Pathol. 185 (2021) 107669, https://doi.org/10.1016/j.jip.2021.107669.

[21] M. Ali, T. Gu, X. Yu, A. Bashir, Z. Wang, X. Sun, N.M. Ashraf, L. Li, Identification of the genes of the plant pathogen *Pseudomonas syringae* MB03 required for the nematicidal activity against *Caenorhabditis elegans* through an integrated approach, Front. Microbiol. 13 (2022) 826962, https://doi.org/10.3389/fmicb.2022.826962.

[22] T. Kaletta, M.O. Hengartner, Finding function in novel targets: *C. elegans* as a model organism, Nat. Rev. Drug Discov. 5 (2006) 387–398, https://doi.org/10.1038/nrd2031.

[23] Q. Li, Q. Yan, J. Chen, Y. He, J. Wang, H. Zhang, Z. Yu, L. Li, Molecular characterization of an ice nucleation protein variant (InaQ) from *Pseudomonas syringae* and the analysis of its transmembrane transport activity in *Escherichia coli*, Int. J. Biol. Sci. 8 (2012) 1097–1108, https://doi.org/10.7150/ijbs.4524.

[24] J. Sambrook, D.W. Russell, Molecular Cloning: a Laboratory Manual, third ed., Cold Spring Harbor Laboratory Press, Cold Spring Harbor, N.Y, 2001.

[25] M. Porta-de-la-Riva, L. Fontrodona, A. Villanueva, J. Cerón, Basic *Caenorhabditis elegans* methods: synchronization and observation, J. Vis. Exp. 64 (2012) e4019, https://doi.org/10.3791/4019.

[26] M.M. Bradford, A rapid and sensitive method for the quantitation of microgram quantities of protein utilizing the principle of protein-dye binding, Anal. Biochem. 72 (1976) 248–254, https://doi.org/10.1006/abio.1976.9999.

[27] J.S. Griffitts, J.L. Whitacre, D.E. Stevens, R.V. Aroian, Bt toxin resistance from loss of a putative carbohydrate-modifying enzyme, Science 293 (2001) 860–864, https://doi.org/10.1126/science.1062441.

[28] A. Paiano, A. Margiotta, M. De Luca, C. Bucci, Yeast two-hybrid assay to identify interacting proteins, Curr Protoc Protein Sci 95 (2019) e70, https://doi.org/10.1002/cpps.70.

[29] M.R. Green, J. Sambrook, J. Total RNA extraction from *Caenorhabditis elegans*, Cold Spring Harb. Protoc. 2020 (2020) 101683, https://doi.org/10.1101/pdb.prot101683.

[30] D.G. Gibson, L. Young, R.Y. Chuang, J.C. Venter, C.A. Hutchison 3rd, H.O. Smith, Enzymatic assembly of DNA molecules up to several hundred kilobases, Nat. Methods 6 (2009) 343–345, https://doi.org/10.1038/nmeth.1318.

[31] J. Zhu, X. Cai, T.L. Harris, M. Gooyit, M. Wood, M. Lardy, K.D. Janda, Disarming *Pseudomonas aeruginosa* virulence factor LasB by leveraging a *Caenorhabditis elegans* infection model, Chem. Biol. 22 (2015) 483–491, https://doi.org/10.1016/j.chembiol.2015.03.012.

[32] D. Conte Jr., L.T. MacNeil, A.J.M. Walhout, C.C. Mello, RNA interference in *Caenorhabditis elegans*, Curr. Protoc. Mol. Biol. 109 (2015) 26.23.21–26.23.30, https://doi.org/10.1002/0471142727.mb2603s109.

[33] K.J. Livak, T.D. Schmittgen, Analysis of relative gene expression data using real-time quantitative PCR and the $2^{-\Delta\Delta CT}$ method, Methods 25 (2001) 402–408, https://doi.org/10.1006/meth.2001.1262.

[34] N. Qin, D. Xu, J. Li, X.W. Deng, COP9 signalosome: discovery, conservation, activity, and function, J. Integr. Plant Biol. 62 (2020) 90–103, https://doi.org/10.1111/jipb.12903.

[35] L. Broday, C.A. Hauser, I. Kolotuev, Z. Ronai, Muscle-epidermis interactions affect exoskeleton patterning in *Caenorhabditis elegans*, Dev. Dyn. 236 (2007) 3129–3136, https://doi.org/10.1002/dvdy.21341.

[36] P. Gerke, A. Keshet, A. Mertenskötter, R.J. Paul, The JNK-like MAPK KGB-1 of *Caenorhabditis elegans* promotes reproduction, lifespan, and gene expressions for protein biosynthesis and germline homeostasis but interferes with hyperosmotic stress tolerance, Cell. Physiol. Biochem. 34 (2014) 1951–1973, https://doi.org/10.1159/000366392.

[37] K. Gieseler, H. Qadota, G.M. Benian, Development, Structure, and Maintenance of *C. elegans* Body Wall Muscle, vol. 2017, WormBook, 2017, pp. 1–59, https://doi.org/10.1895/wormbook.1.81.2.

[38] P. Smith, W.M. Leung-Chiu, R. Montgomery, A. Orsborn, K. Kuznicki, E. Gressman-Coberly, L. Mutapcic, K. Bennett, The GLH proteins, *Caenorhabditis elegans* P granule components, associate with CSN-5 and KGB-1, proteins necessary for fertility, and with ZYX-1, a predicted cytoskeletal protein, Dev. Biol. 251 (2002) 333–347, https://doi.org/10.1006/dbio.2002.0832.

[39] D.S. Yoon, D.S. Cha, Y. Choi, J.W. Lee, M.H. Lee, MPK-1/ERK is required for the full activity of resveratrol in extended lifespan and reproduction, Aging Cell 18 (2019) e12867, https://doi.org/10.1111/acel.12867.

[40] R.K. Miller, H. Qadota, T.J. Stark, K.B. Mercer, T.S. Wortham, A. Anyanful, G.M. Benian, CSN-5, a component of the COP9 signalosome complex, regulates the levels of UNC-96 and UNC-98, two components of M-lines in *Caenorhabditis elegans* muscle, Mol. Biol. Cell 20 (2009) 3608–3616, https://doi.org/10.1091/mbc.e09-03-0208.

[41] A.I.M. Salah Ud-Din, A. Roujeinikova, Methyl-accepting chemotaxis proteins: a core sensing element in prokaryotes and archaea, Cell. Mol. Life Sci. 74 (2017) 3293–3303, https://doi.org/10.1007/s00018-017-2514-0.

[42] C. Geng, Y. Liu, M. Li, Z. Tang, S. Muhammad, J. Zheng, D. Wan, D. Peng, L. Ruan, M. Sun, Dissimilar crystal proteins Cry5Ca1 and Cry5Da1 synergistically act against *Meloidogyne incognita* and delay Cry5Ba-Based nematode resistance, Appl. Environ. Microbiol. 83 (2017) e03505–e03516, https://doi.org/10.1128/AEM.03505-16.

[43] T. Kim, K. Hofmann, A.G. von Arnim, D.A. Chamovitz, PCI complexes: pretty complex interactions in diverse signaling pathways, Trends Plant Sci. 6 (2001) 379–386, https://doi.org/10.1016/s1360-1385(01)02015-5.

[44] S.N. Zhang, D.S. Pei, J.N. Zheng, The COP9 signalosome subunit 6 (CSN6): a potential oncogene, Cell Div. 8 (2013) 14, https://doi.org/10.1186/1747-1028-8-14.

[45] M.S. Vijayabaskar, S. Vishveshwara, Insights into the fold organization of TIM barrel from interaction energy based structure networks, PLoS Comput. Biol. 8 (2012) e1002505, https://doi.org/10.1371/journal.pcbi.1002505.

[46] G.H. Braus, S. Irniger, O. Bayram, Fungal development and the COP9 signalosome, Curr. Opin. Microbiol. 13 (2010) 672–676, https://doi.org/10.1016/j.mib.2010.09.011.

[47] A. Sandhu, D. Badal, R. Sheokand, S. Tyagi, V. Singh, Specific collagens maintain the cuticle permeability barrier in *Caenorhabditis elegans*, Genetics 217 (2021) iyaa047, https://doi.org/10.1093/genetics/iyaa047.